Triple-Mode Bandpass Filters on CSRR-Loaded Substrate Integrated Waveguide Cavities

Zheng Liu, *Student Member, IEEE*, Gaobiao Xiao, *Member, IEEE*, and Lei Zhu, *Fellow, IEEE*

***Abstract*— In this paper, a novel approach is proposed to design and explore a class of triple-mode bandpass filters on substrate integrated waveguide (SIW) structure. Two degenerate modes of an SIW rectangular cavity and one resonant mode of a complementary split-ring resonator (CSRR) are employed to implement these filters. As the primary advantage, the CSRR mode is utilized instead of the fundamental mode of the SIW cavity to provide us with an attractive capacity in easily controlling the frequency band of the designed SIW filters through the dimensions of this CSRR. Moreover, the positions of transmission zeros can be properly adjusted by the metallic vias. Finally, three examples of SIW multimode bandpass filters are designed, fabricated, and tested to verify the effectiveness of the proposed approach. The measured results are found in good agreement with the simulated ones, showing that these filters have achieved high out-of-band rejection and sharp skirt selectivity.**

***Index Terms*— Bandpass filter, complementary split ring resonators (CSRRs), substrate integrated waveguide (SIW), triple-mode resonance.**

I. Introduction

MICROWAVE filters on the substrate integrated waveguide (SIW) structure have been attracting much research interest, and various kinds of SIW bandpass filters with different filtering characteristics have been recently published [1]–[6]. One of these research hotspots is the design and synthesis of the so-called multimode SIW filters. In this context, these multimode filters can achieve elliptic or quasi-elliptic responses with improved out-of-band rejection and sharpened skirt selectivity. Compared with the conventional filters with a few cascaded resonators, these multimode filters can greatly reduce their whole size due to the usage of multiple resonant modes in a single SIW cavity. Therefore, these multimode SIW filters have been widely employed in various applications, such as satellite and cellular phone base stations.

Thus far, the dual-mode SIW filters have been extensively investigated, mainly based on two degenerate resonant modes in oversized circular and square cavities. However, these dual-mode SIW filters unfortunately suffer from narrow band and poor out-of-band rejection due to transmission zeros (TZs) less than two [7]–[9]. In order to improve the frequency response of these filters, the triple-mode filters on SIW are studied as reported in [10]–[18]. In [10], the first planar triple-mode filter is reported and it consists of a dual-mode square-loop resonator and a resonant metal cavity. However, its multilayer configuration may restrict its application in practice. Single-layer planar triple-mode filters are reported in [13] and [14], and they are implemented by incorporating a dual-mode microstrip resonator in a single-mode SIW cavity. In [15]–[17], a few other triple-mode SIW filters are designed using the fundamental mode and two higher order degenerate modes within an SIW cavity. As usual, the resonant frequency of the fundamental mode is far away from those of its two higher order degenerate modes. By properly increasing the fundamental resonant mode toward two higher order modes, the three resonant modes can be reallocated in proximity to each other, thereby constructing the three-pole passband as desired. Although these filters have good performance, their operating bandwidth is hardly tunable, thus restraining the flexibility in practical circuit design. In [18], a triple-mode SIW filter using a few high-order resonant modes is reported, but it suffers from the emergence of an unexpected parasitic passband near the desired frequency band. We have proposed a so-called multiple-mode resonator (MMR) filter technology to design filters [20], [21]. MMRs have been realized in a metal cavity by creating degeneration modes in a single resonator. Then the filters can be constructed by analyzing and exciting these degeneration modes without resort to the coupling matrix [10], [11], [15], [17]. In this paper, the MMR technology is further to extended to directly design SIW triple-mode filters.

On the other hand, the complementary split-ring resonators (CSRRs) have recently drawn increasing attention to design of various bandpass filters. Similar to the split-ring resonators, CSRRs can provide a negative effective permittivity in the vicinity of its resonant frequency. The CSRRs and their equivalent circuit models have been comprehensively studied in [22] and [23]. These CSRRs can be integrated with SIWs to form up various kinds of filters as reported in [7] and [24]–[27].

In this paper, the CSRR is used as a resonator to work together with a dual-mode SIW rectangular cavity to constitute a new triple-mode SIW filter. As an advantage of using the CSRR instead of the fundamental mode in an SIW cavity, the resonant frequency of the CSRR mainly depends on its own size, thus providing us with another degree of freedom to

Manuscript received January 8, 2016; revised May 8, 2016; accepted May 23, 2016. Date of publication June 29, 2016; date of current version July 14, 2016. This work was supported in part by the Fundo para o Desenvolvimento das Ciências e da Tecnologia through the Macao Science and Technology Development Fund under Grant 051/2014/A1 and in part by the Multi-Year Research Grant through the University of Macau, Macau, China, under Grant MYRG2014-00079-FST. Recommended for publication by Associate Editor D. G. Kam upon evaluation of reviewers' comments.

Z. Liu and G. Xiao are with the Key Laboratory of Ministry of Education of Design and Electromagnetic Compatibility of High Speed Electronic Systems, Shanghai Jiao Tong University, Shanghai 200000, China (e-mail: lzheng_2012@sjtu.edu.cn).

L. Zhu is with the Department of Electrical and Computer Engineering, Faculty of Science and Technology, University of Macau, Macau 999078, China.

Color versions of one or more of the figures in this paper are available online at http://ieeexplore.ieee.org.

Digital Object Identifier 10.1109/TCPMT.2016.2574562

control the operating bandwidth of the designed SIW filters. Meanwhile, three TZs can be excited and their locations can be adjusted with proper perturbation to helpfully improve the out-of-band rejection characteristics. In order to verify the proposed method, two examples of triple-mode SIW filters with different bandwidths and frequency responses are proposed and designed. Finally, a two-stage filter with high out-of-band rejection and sharp skirt selectivity is realized by cascading the two previously designed SIW filters.

The remainder of this paper is organized as follows. The three modes and the excitation approach within an SIW cavity are analyzed in Section II. In Section III, the quality factors and Q-factors of SIW cavity loaded with and without CSRR are extracted to provide the comparison in insertion loss between them. Three examples of SIW multimode filters are designed with the proposed method, and then fabricated for experimental validation in Section IV. Finally, the conclusion is given in Section V.

II. Excitation of Three Modes Within SIW Cavity

As proved in [28], only the TE_{n0} modes can exist in SIW due to its electrically thin thickness. Thus, the TE_{101} mode can be considered as the fundamental mode of an SIW square cavity, whereas the two degenerate modes, i.e., TE_{102} and TE_{201} modes, are the lowest higher order modes. For the TE modes, their electric field is perpendicular to the top and bottom metal surfaces in an SIW cavity, while the magnetic field is parallel to these two surfaces and perpendicular to the left- and right-side metal walls. Therefore, the electric field of TE_{101} mode reaches to its maximum at the center of the cavity, while the two degenerate modes, i.e., TE_{102} and TE_{201} modes, vanish there. As studied in [22] and [23], the CSRR essentially behaves as an electric dipole and requires an axial electric excitation when the CSRR is etched on the top metal of the cavity. In this case, the CSRR can be excited by the TE_{101} mode within the SIW cavity.

Fig. 1(a) depicts the geometrical configuration of the SIW cavity with a CSRR etched on its top metal. The square-shaped CSRR is chosen due to its good suitability in alignment. Fig. 1(b)–(d) gives the electric field distributions of the three above-mentioned resonant modes, within this cavity, which are employed herein to design a class of alternative triple-mode filters. It can be clearly seen that the electric field of CSRR- mode mainly concentrates on its slots. For the TE_{102} and TE_{201} modes, their electric fields almost keep their respective manner with receiving any significant influence from the CSRR.

It is well known as studied in [1] and [29] that the resonant characteristics of a cavity resonator tremendously depend on the coupling position of feed lines at the input and output ports. The concerned mode chart of an SIW cavity loaded with a CSRR under two different weak couplings is plotted in the inset of Fig. 2. The resonant frequency of the CSRR mode is denoted by f_1, while f_2 stands for the resonant frequency of TE_{201} mode within the cavity. It is noted that the two degenerate modes, i.e., TE_{102} and TE_{201} modes, are perfectly merged due to no perturbation to be introduced at this stage.

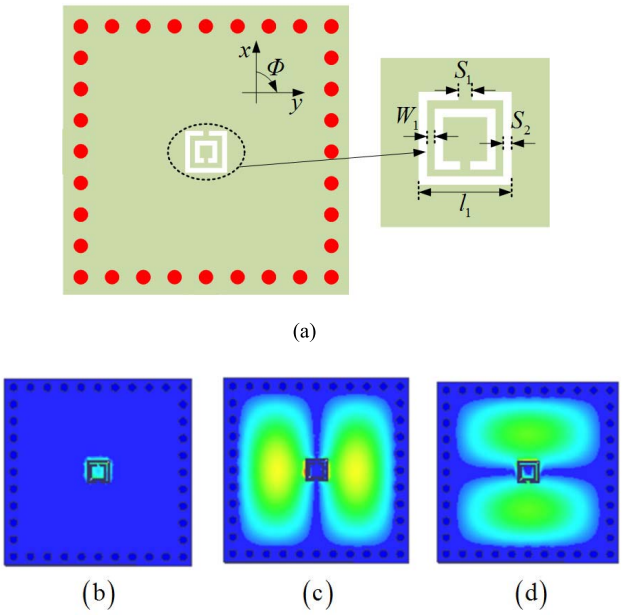

Fig. 1. (a) Configuration of the CSRR etched on the top metal of an SIW cavity. (b)–(d) Field distributions in CSRR-loaded SIW cavity for three distinct modes: CSRR mode, TE_{102} mode, and TE_{201} mode, respectively.

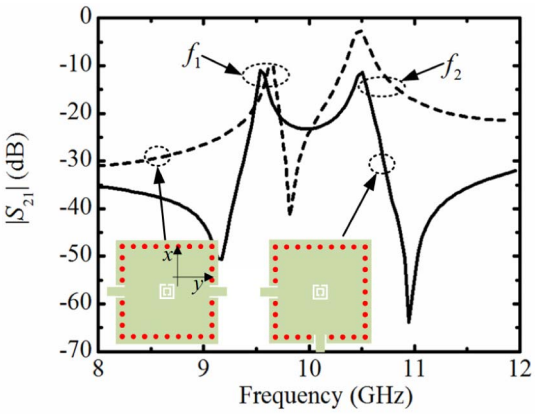

Fig. 2. Resonant characteristics of the proposed SIW cavity loaded with a CSRR under two different excitations.

As can be observed from Fig. 2, the feed lines at the input and output ports are symmetrical along the x-axis, so a TZ supposes to appear between f_1 and f_2. Under this condition, the triple-mode filter cannot be implemented and the out-of-band rejection is yet poor. However, when the feed lines are placed to be orthogonal to each other, the TZ between f_1 and f_2 vanishes, and instead, a pair of TZs appear in the lower and upper operating bands. These two out-of-band TZs are definitely helpful for design of an alternative multimode SIW filter with sharp skirt selectivity and high out-of-band rejection.

As investigated in [22], the resonant frequency of the CSRR mode mainly depends on its own size. Therefore, we can expect that this resonant frequency tends to be ranged between f_1 and f_2, and its value can be properly tuned with virtue of the CRSS dimension. Fig. 3(a) and (b) presents the variation

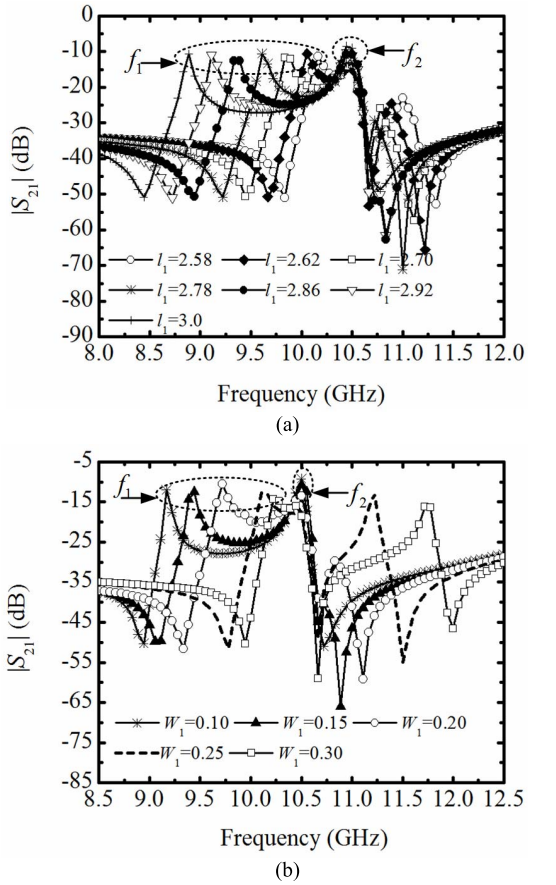

Fig. 3. (a) Resonant frequencies of CSRR mode versus l_1 under weak coupling. (b) Variation in resonant frequency as a function of W_1 (unit: mm).

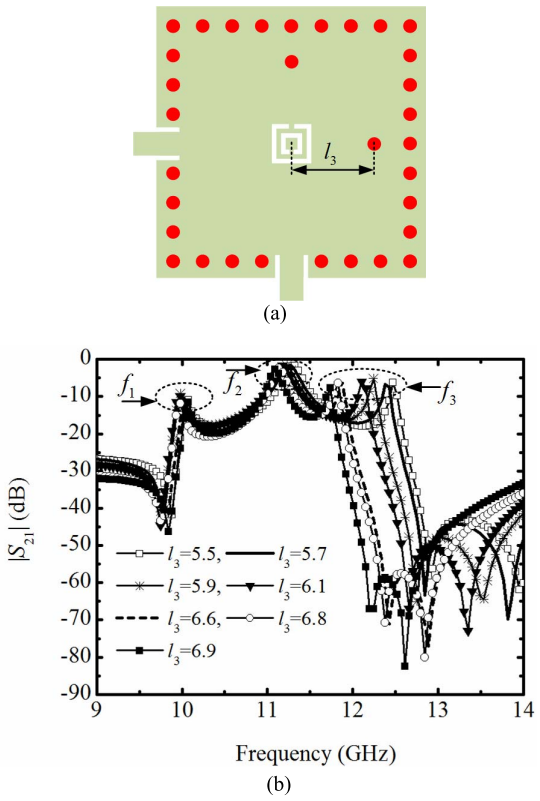

Fig. 4. (a) Configuration of SIW cavity with perturbation metallic vias. (b) Simulated magnitude of S_{21} under different values of l_3 (unit: mm).

of the resonant frequencies versus the parameters l_1 and W_1 of the CRSS-loaded SIW cavity in Fig. 1(a). The orthogonal input/output feed lines are arranged to be linked with their respective degenerate modes via weak coupling.

From Fig. 3(a), we can see that under other CRSS parameters to be fixed, the resonant frequency f_1 of the CSRR mode in the cavity decreases with the increase in l_1, while f_2 remains almost the same. The reason is that the electric field of TE_{201} mode is null at the center of an SIW rectangular cavity, and thus its resonant frequency is hardly affected by the CSRR. Fig. 3(b) provides a similar variation tendency for f_1 and f_2. With the increase in W_1, f_1 moves downward, while f_2 remains unchanged. Thus, the frequency range or spacing between f_1 and f_2 can be controlled by changing the dimensions of CSRR. This property is useful for us to control the operating bandwidth of our proposed multimode CRSS-loaded SIW bandpass filter.

Now, let us excite the third mode of this cavity, i.e., the TE_{102} mode, whose resonant frequency is denoted by f_3 in Fig. 4(b). In this context, two metallic vias are perpendicularly inserted in the cavity as illustrated in Fig. 4(a). These two perturbation vias are both located away from the center of the cavity with a distance l_3.

The variation of these three resonant frequencies is plotted in Fig. 4(b) as a function of l_3. As l_3 increases, the value of f_3 tends to tremendously move downward. The value of f_2 is slightly affected by l_3, but its variation range is less than that of f_3. Meanwhile, the value of f_1 almost remains unchanged in this process. Thus, the operating bandwidth between f_2 and f_3 can be effectively adjustable and controllable.

III. Q-Factor of CSRR-Loaded SIW Cavity

As a common concern, the CSRR etched on the top metal of the SIW cavity may cause radiation loss so that the insertion loss of the designed bandpass filter may deteriorate seriously. For this purpose, the insertion loss of a cavity filter, denoted by insertion loss (IL), can be characterized and analyzed in terms of external and unloaded Q-factors, i.e., Q_e and Q_0, such that

$$\mathrm{IL(dB)} = -20\log\left(\frac{Q_0}{(Q_0+Q_e)}\right). \tag{1}$$

First, let us try to extract the unloaded Q-factors of the TE_{201} mode and TE_{102} mode within an SIW square cavity. Because the resonant characteristics of the two degenerate modes are the same, only the TE_{201} mode is discussed following the work in [7]. Herein, the value of Q_0 for the CSRR-loaded SIW cavity is numerically extracted with virtue to the electromagnetic simulator, namely, High frequency simulator structure (HFSS).

In order to obtain the value of Q_e, the classical slot transitions are used to achieve the desired critical coupling and impedance matching between the feed lines and the SIW cavity. It is worthwhile to note that the external Q-factor,

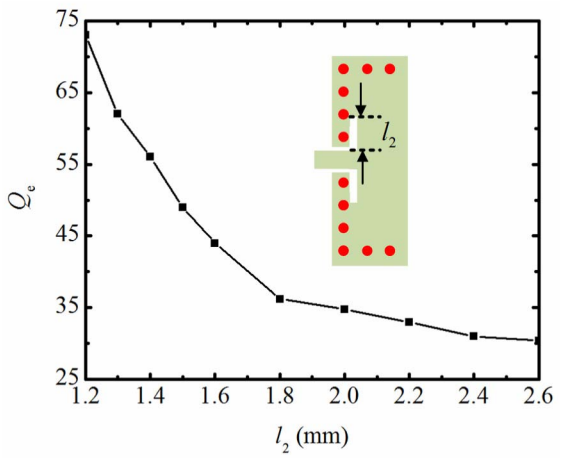

Fig. 5. Extracted external Q-factor as a function of l_2.

TABLE I
INSERTION LOSS OF SIW CAVITY WITH/WITHOUT CSRR

	TE_{201}		Q_e	IL (dB)
	f_0 (GHz)	Q_0		
Cavity	10.85	649.83	35	0.45
Cavity with CSRR	10.67	640.12	35	0.46

Q_e, is also extracted for the same mode of unloaded Q-factor, i.e., the TE_{201} mode [7], [17]. Fig. 6 depicts the configuration of this slot transition as used in [30]–[32]. According to the coupled-resonator theory, Q_e can be numerically obtained by simulating a doubly loaded resonator using the following formula from [24] and [29]:

$$Q_e = \frac{2f_0}{\Delta f_{3\,\mathrm{dB}}} \tag{2}$$

where f_0 is the resonant frequency in the SIW cavity resonator and $\Delta f_{3\,\mathrm{dB}}$ is the absolute bandwidth under 3-dB definition.

Fig. 5 depicts the extracted Q_e as a function of the slot length l_2 in the microstrip-to-SIW transition. As l_2 is enlarged, Q_e is found to gradually fall down.

After the values of Q_e and Q_0 are derived, the insertion loss (IL) can be calculated using (1), and their values are tabulated in Table I.

It is found that the value of unloaded Q-factor for the TE_{201} mode varies by 1.5% as the CSRR is etched on the top metal of the cavity. The insertion loss is increased by only 0.01 dB at the resonant frequency, so we can figure out that any extra loss by CRSS can be neglected. This phenomenon can be explained by the fact that the electric field intensity of the two degenerate modes basically vanishes near the center of the cavity. As such, the CSRR cannot be excited by these two degenerate modes, thereby causing very low radiation loss from this loaded cavity.

IV. MULTIMODE FILTER ON CRSS-LOADED SIW CAVITY

In order to verify the accuracy of our proposed method, two triple-mode SIW filters with different operating bandwidths and frequency responses are proposed and designed in this section. Afterward, a multimode filter with high out-of-band rejection and sharp skirt selectivity is presented by cascading these two designed filters. The substrate used in this paper is the Taconic TLX with a thickness of 1.0 mm, a relative permittivity of 2.55, and a dielectric loss tangent of 0.0019. In the designed SIW filters, all the metallic vias have the same diameter of 1.0 mm. The via-to-via spacing in the two side walls of the SIW cavity is readily set as 2.0 mm.

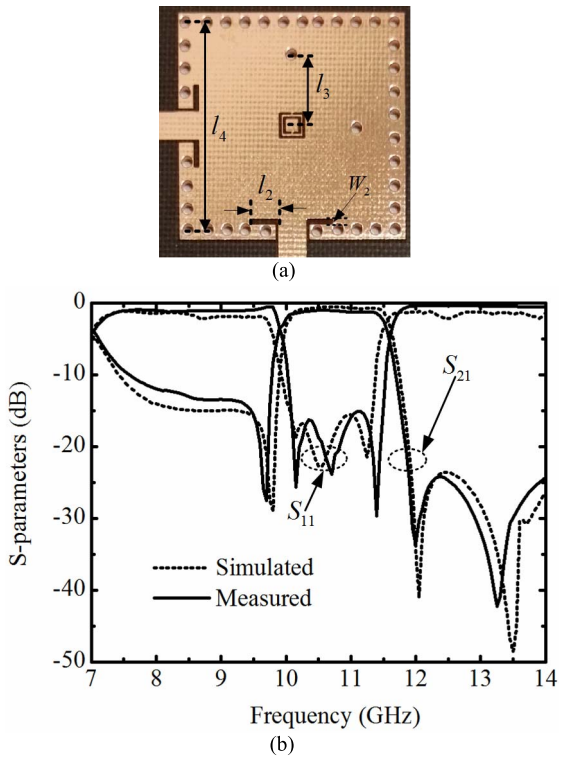

Fig. 6. (a) Photography of the fabricated triple-mode filter A. (b) Simulated and measured scattering parameters of the designed filter A.

A. Example A

First of all, a triple-mode bandpass filter on CRSS-loaded SIW cavity with high out-of-band rejection in the upper frequency band is designed and fabricated. Its photograph is depicted in Fig. 6(a). The optimized parameters are obtained as $l_1 = 2.68$ mm, $S_1 = 0.30$ mm, $S_2 = 0.20$ mm, $W_1 = 0.20$ mm, $l_4 = 20$ mm, $l_3 = 6.85$ mm, $W_2 = 0.40$ mm, and $l_2 = 2.45$ mm.

The measured and simulated scattering parameters are plotted in Fig. 6(b), showing good agreement between them. The measured central frequency is 10.8 GHz, and the 3-dB absolute bandwidth is about 1.8 GHz. The measured insertion loss including the effect of nonideal Subminiature version A (SMA) connectors is 1.5 dB, and it is 0.5 dB slightly larger than the simulated one. The measured in-band return loss is 15 dB, and slight discrepancies between the simulated and the measured ones in the lower and upper out-of-band rejection are primarily caused by some unexpected tolerance in fabrication and measurement. Three TZs can be observed to

TABLE II
COMPARISON WITH OTHER REPORTED SIW-BASED TRIPLE-MODE FILTERS

Filters	FBW	Zeros		BW tunable
		lower	upper	
[7]	8%	1	2	/
[11]	48%	0	1	/
[12]	15.2%	0	1	/
[13]	4%	1	1	/
[14]	13%	0	1	/
[15]	14%	0	2	/
[16]	15%	0	3	/
[17]	9%	0	3	/
Example-A	**16.5%**	**1**	**2**	**Yes**
Example-B	**9.7%**	**2**	**1**	**Yes**

emerge at 9.7, 11.9, and 13.2 GHz, respectively, and high out-of-band rejection in the upper band and sharp skirt selectivity have been achieved. Due to the parasitical passing band, which is caused by the fundamental mode of SIW cavity, TE_{101} mode, the out-of-band rejection in the lower frequency is about 10 dB from 7.8 to 10 GHz, and is inferior to the one in the upper band. Table II is prepared to compare the designed CRSS-loaded SIW filter with other reported triple-mode SIW filters in terms of various critical electrical parameters.

B. Example B

Second, a triple-mode bandpass filter on CRSS-loaded SIW cavity with narrow bandwidth is designed. It is formed up by decreasing the external dimensions of CSRR, i.e., l_1 in Fig. 1(a), under other parameters to be remained.

The designed filter in Example A has a single TZ in the lower band and two TZs in the upper band. Therefore, its out-of-band rejection in the lower band is inferior to that in its upper band, because the unwanted fundamental mode exists in this SIW cavity. In order to improve the out-of-band rejection in the lower band, one additional TZ in the upper band can be moved down to the lower band by properly changing the positions of the perturbation metallic vias.

After the design of this second filter is accomplished, a filter circuit is fabricated and tested using the same substrate as before. Fig. 7(a) shows the photography of this fabricated filter, and Fig. 7(b) provides its simulated and measured results. In this filter, the perturbation metallic vias are located in the diagonal positions so as to excite the two degenerate modes of the SIW cavity, i.e., the TE_{102} and TE_{201} modes. The final optimized parameters for this filter are derived as $l_1 = 2.56$ mm, $S_1 = 0.30$ mm, $S_2 = 0.20$ mm, $W_1 = 0.20$ mm, $l_3 = 8.68$ mm, $l_{21} = 2.05$ mm, $l_{22} = 1.55$ mm, and $W_2 = 0.40$ mm.

Again, the simulated scattering parameters agree well with the measured ones. The insertion loss is about 1.4 dB, and its 3-dB frequency band is ranged from 10.25 to 11.3 GHz. The return loss is better than 15 dB in its desired passband. Compared with Example A, its fractional bandwidth of this filter is somehow changed by about 6.8%. Three TZs appear at 9.5, 9.89, and 12.1 GHz, respectively. As expected, one TZ has been moved from the upper band to the lower band

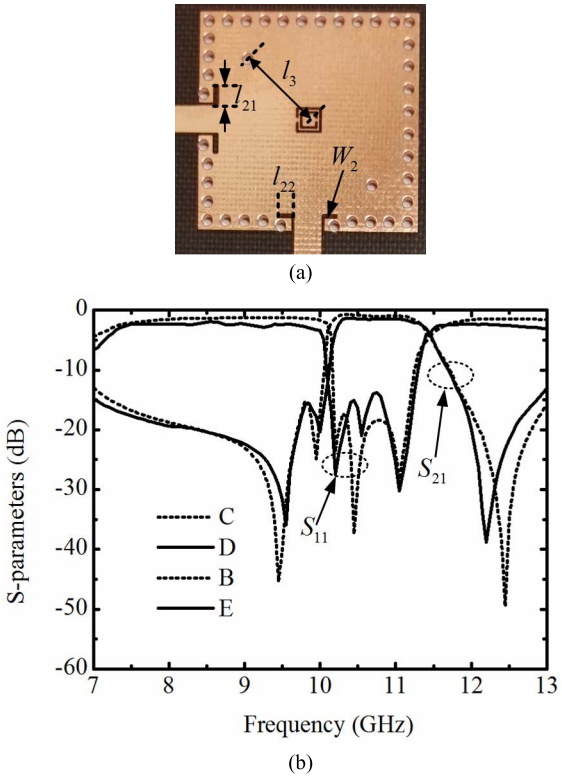

Fig. 7. (a) Photography of the fabricated triple-mode filter B. (b) Simulated and measured scattering parameters of the designed filter.

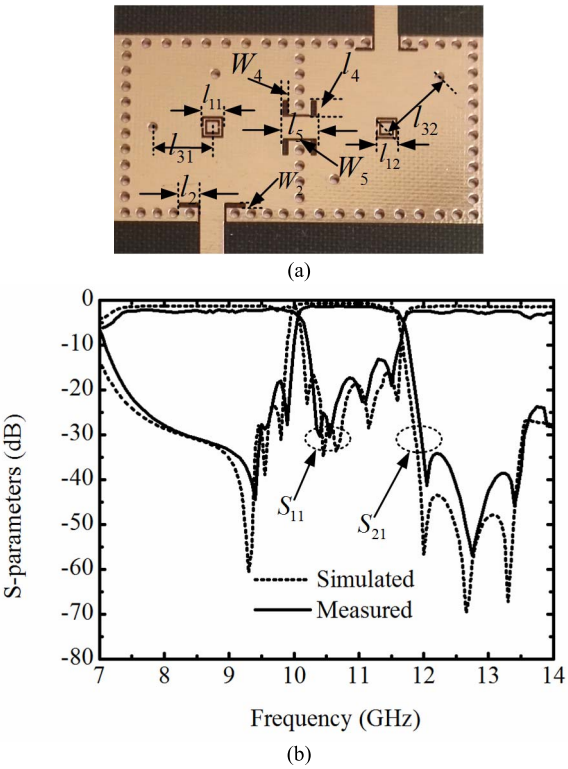

Fig. 8. (a) Photography of the final fabricated filter with two cascaded multimode filters. (b) Simulated and measured scattering parameters.

by adjusting the positions of metallic vias. Compared with the results of Example A, improved stopband characteristics in the lower stopband have been obtained. The out-of-band

rejection in the lower band is about 15 dB in the frequency range 7.2–10 GHz, while the out-of-band rejection in the upper band deteriorates. Small discrepancies between the simulated and the measured return losses may be caused by the tolerance in fabrication and measurement tolerances, as well as the parasitic effect of SMA connectors.

C. Example C

In order to improve the out-of-band rejection in both the lower and upper bands, the third filter, namely, Example C, is designed by cascading the two previously designed filters in Examples A and B toward enhanced filtering selectivity. Fig. 8(a) shows the photography of this high-order multi-mode SIW filter. Slot coupling is employed to achieve the desired coupling strength between the two SIW cavities. After simulation and optimization is executed via HFSS, all the dimensions of this filter are determined as $l_{11} = 2.50$ mm, $l_{12} = 2.62$ mm, $S_1 = 0.30$ mm, $S_2 = 0.20$ mm, $W_1 = 0.20$ mm, $l_2 = 2.05$ mm, $W_2 = 0.50$ mm, $l_{31} = 8.85$ mm, $l_{32} = 6.85$ mm, $l_4 = 1.90$ mm, $W_4 = 0.65$ mm, $l_5 = 3.90$ mm, and $W_5 = 0.20$ mm.

The simulated and measured scattering parameters are plotted in Fig. 8(b), and they are found in good agreement with each other. In particular, we can see that the high out-of-band rejection and sharp skirt selectivity have been obtained with the help of three TZs in both the lower and upper bands. Although the parasitical passing band exists, the out-of-band rejection is better than 20 dB from 7.5 to 10 GHz. Meanwhile, in the upper band, its value is larger than 20 dB. Thus, this cascaded filter has achieved skirt selectivity and high out-of-band rejection in both the lower and upper bands. In addition, the insertion loss is found as about 1.8 dB, the return loss is better than 15 dB, and the fractional bandwidth is about 15.7%.

V. Conclusion

In this paper, a class of triple-mode filters on the SIW rectangular cavity loaded with CSRR is proposed. On the one hand, the CRSS on SIW can dominate and adjust the operating band of these filters, thus holding the good flexibility in the practical design. On the other hand, the frequency responses of these filters can be tuned and reshaped with virtue of the perturbation metallic vias, thus improving the out-of-band rejection and skirt selectivity. The effectiveness of the method has been verified in experiment by three designed triple-mode CRSS-loaded SIW bandpass filters.

References

[1] X.-P. Chen and K. Wu, "Substrate integrated waveguide filters: Design techniques and structure innovations," *IEEE Microw. Mag.*, vol. 15, no. 6, pp. 121–133, Sep./Oct. 2014.

[2] X.-P. Chen and K. Wu, "Self-packaged millimeter-wave substrate integrated waveguide filter with asymmetric frequency response," *IEEE Trans. Compon., Packag., Manuf. Technol.*, vol. 2, no. 5, pp. 775–782, May 2012.

[3] B. Y. El Khatib, T. Djerafi, and K. Wu, "Substrate-integrated waveguide vertical interconnects for 3-D integrated circuits," *IEEE Trans. Compon., Packag., Manuf. Technol.*, vol. 2, no. 9, pp. 1526–1535, Sep. 2012.

[4] S.-W. Wong, R. S. Chen, K. Wang, Z.-N. Chen, and Q.-X. Chu, "U-shape slots structure on substrate integrated waveguide for 40-GHz bandpass filter using LTCC technology," *IEEE Trans. Compon., Packag., Manuf. Technol.*, vol. 5, no. 1, pp. 128–134, Jan. 2015.

[5] W. Shen, W.-Y. Yin, X.-W. Sun, and L.-S. Wu, "Substrate-integrated waveguide bandpass filters with planar resonators for system-on-package," *IEEE Trans. Compon., Packag., Manuf. Technol.*, vol. 3, no. 2, pp. 253–261, Feb. 2013.

[6] C. Jin, R. Li, S. Hu, S. Zhang, K. F. Chang, and B. Zheng, "Self-shielded circularly polarized antenna-in-package based on quarter mode substrate integrated waveguide subarray," *IEEE Trans. Compon., Packag., Manuf. Technol.*, vol. 4, no. 3, pp. 392–399, Mar. 2014.

[7] L.-S. Wu, X.-L. Zhou, Q.-F. Wei, and W.-Y. Yin, "An extended doublet substrate integrated waveguide (SIW) bandpass filter with a complementary split ring resonator (CSRR)," *IEEE Microw. Wireless Compon. Lett.*, vol. 19, no. 12, pp. 777–779, Dec. 2009.

[8] H. J. Tang, W. Hong, J.-X. Chen, G. Q. Luo, and K. Wu, "Development of millimeter-wave planar diplexers based on complementary characters of dual-mode substrate integrated waveguide filters with circular and elliptic cavities," *IEEE Trans. Microw. Theory Techn.*, vol. 55, no. 4, pp. 776–782, Apr. 2007.

[9] R. Q. Li, X. H. Tang, and F. Xiao, "Substrate integrated waveguide dual-mode filter using slot lines perturbation," *Electron. Lett.*, vol. 46, no. 12, pp. 845–846, Jun. 2010.

[10] C. Lugo and J. Papapolymerou, "Planar realization of a triple-mode bandpass filter using a multilayer configuration," *IEEE Trans. Microw. Theory Techn.*, vol. 55, no. 2, pp. 296–301, Feb. 2007.

[11] R. S. Chen, S.-W. Wong, L. Zhu, and Q.-X. Chu, "Wideband bandpass filter using u-slotted substrate integrated waveguide (SIW) cavities," *IEEE Microw. Wireless Compon. Lett.*, vol. 25, no. 1, pp. 1–3, Jan. 2015.

[12] F. Ren, W. Hong, and K. Wu, "Design and implementation of an SIW triple-mode filter," in *Proc. 3rd Asia-Pacific Conf. Antennas Propag.*, Harbin, China, Jul. 2014, pp. 1228–1230.

[13] L.-S. Wu, J.-F. Mao, W. Shen, and W.-Y. Yin, "An extended doublet bandpass filter implemented with microstrip resonator and substrate integrated waveguide cavity," in *Proc. Asia-Pacific Microw. Conf.*, Yokohama, Japan, Dec. 2010, pp. 251–254.

[14] W. Shen, W.-Y. Yin, X.-W. Sun, and J.-F. Mao, "Compact substrate integrated waveguide (SIW) transversal filter with triple-mode microstrip resonator," in *Proc. Asia-Pacific Microw. Conf.*, Yokohama, Japan, Dec. 2010, pp. 1875–1878.

[15] X.-C. Zhu *et al.*, "Design and implementation of a triple-mode planar filter," *IEEE Microw. Wireless Compon. Lett.*, vol. 23, no. 5, pp. 243–245, May 2013.

[16] M. Rezaee and A. R. Attari, "Realisation of new single-layer triple-mode substrateintegrated waveguide and dual-mode half-mode substrate-integrated waveguide filters using a circular shape perturbation," *IET Microw., Antennas Propag.*, vol. 7, no. 14, pp. 1120–1127, Nov. 2013.

[17] D.-D. Zhang, L. Zhou, L.-S. Wu, L.-F. Qiu, W.-Y. Yin, and J.-F. Mao, "Novel bandpass filters by using cavity-loaded dielectric resonators in a substrate integrated waveguide," *IEEE Trans. Microw. Theory Techn.*, vol. 62, no. 5, pp. 1173–1182, May 2014.

[18] Y. Dong, W. Hong, H. Tang, J. Chen, and K. Wu, "Planar realization of a *Q*-band triple-mode filter using high-order resonances," *Microw. Opt. Technol. Lett.*, vol. 51, no. 3, pp. 600–603, Mar. 2009.

[19] K.-S. Chin, C.-C. Chang, C.-H. Chen, Z. Guo, D. Wang, and W. Che, "LTCC multilayered substrate-integrated waveguide filter with enhanced frequency selectivity for system-in-package applications," *IEEE Trans. Compon., Packag., Manuf. Technol.*, vol. 4, no. 4, pp. 664–672, Apr. 2014.

[20] L. Zhu, S. Sun, and W. Menzel, "Ultra-wideband (UWB) bandpass filters using multiple-mode resonator," *IEEE Microw. Wireless Compon. Lett.*, vol. 15, no. 11, pp. 796–798, Nov. 2005.

[21] S. W. Wong and L. Zhu, "EBG-embedded multiple-mode resonator for UWB bandpass filter with improved upper-stopband performance," *IEEE Microw. Wireless Compon. Lett.*, vol. 17, no. 6, pp. 421–423, Jun. 2007.

[22] J. D. Baena *et al.*, "Equivalent-circuit models for split-ring resonators and complementary split-ring resonators coupled to planar transmission lines," *IEEE Trans. Microw. Theory Techn.*, vol. 53, no. 4, pp. 1451–1461, Apr. 2005.

[23] Y. D. Dong, T. Yang, and T. Itoh, "Substrate integrated waveguide loaded by complementary split-ring resonators and its applications to miniaturized waveguide filters," *IEEE Trans. Microw. Theory Techn.*, vol. 57, no. 9, pp. 2211–2223, Sep. 2009.

[24] Y. Dong, C.-T. M. Wu, and T. Itoh, "Miniaturised multi-band substrate integrated waveguide filters using complementary split-ring resonators," *IET Microw., Antennas Propag.*, vol. 6, no. 6, pp. 611–620, Apr. 2011.
[25] Q.-L. Zhang, W.-Y. Yin, S. He, and L.-S. Wu, "Compact substrate integrated waveguide (SIW) bandpass filter with complementary split-ring resonators (CSRRs)," *IEEE Microw. Wireless Compon. Lett.*, vol. 20, no. 8, pp. 426–428, Aug. 2010.
[26] W. Che, C. Li, K. Deng, and L. Yang, "A novel bandpass filter based on complementary split rings resonators and substrate integrated waveguide," *Microw. Opt. Technol. Lett.*, vol. 50, no. 3, pp. 699–701, Mar. 2008.
[27] K. Deng, Z. Guo, C. Li, and W. Che, "A compact planar bandpass filter with wide out-of-band rejection implemented by substrate-integrated waveguide and complementary split-ring resonator," *Microw. Opt. Technol. Lett.*, vol. 53, no. 7, pp. 1483–1487, Jul. 2011.
[28] F. Xu and K. Wu, "Guided-wave and leakage characteristics of substrate integrated waveguide," *IEEE Trans. Microw. Theory Techn.*, vol. 53, no. 1, pp. 66–73, Jan. 2005.
[29] D. M. Pozar, *Microwave Engineering*, 4th ed. New York, NY, USA: Wiley, Nov. 2012.
[30] R.-Y. Fang, C.-F. Liu, and C.-L. Wang, "Compact and broadband CB-CPW-to-SIW transition using stepped-impedance resonator with 90°-bent slot," *IEEE Trans. Compon., Packag., Manuf. Technol.*, vol. 3, no. 2, pp. 247–252, Feb. 2013.
[31] N. Ghassemi, I. Boudreau, D. Deslandes, and K. Wu, "Millimeter-wave broadband transition of substrate integrated waveguide on high-to-low dielectric constant substrates," *IEEE Trans. Compon., Packag., Manuf. Technol.*, vol. 3, no. 10, pp. 1764–1770, Oct. 2013.
[32] Z. Kordiboroujeni and J. Bornemann, "New wideband transition from microstrip line to substrate integrated waveguide," *IEEE Trans. Microw. Theory Techn.*, vol. 62, no. 12, pp. 2983–2989, Dec. 2014.

Zheng Liu (S'12) was born in Shandong, China, in 1984. He is currently pursuing the Ph.D. degree with Shanghai Jiao Tong University, Shanghai, China.

He was an Exchange Student with the University of Macau, Macau, China, from 2014 to 2015. His current research interests include microwave and millimeter-wave passive and active components and circuits.

Gaobiao Xiao (M'02) received the B.S. degree from the Huazhong University of Science and Technology, Wuhan, China, in 1988, the M.S. degree from the National University of Defense Technology, Changsha, China, in 1991, and the Ph.D. degree from Chiba University, Chiba, Japan, in 2002.

He was with Hunan University, Changsha, from 1991 to 1997. Since 2004, he has been a Faculty Member with the Department of Electronic Engineering, Shanghai Jiao Tong University, Shanghai, China. His current research interests include numerical methods in electromagnetic fields, coupled thermoelectromagnetic analysis, microwave filter designs, fiber-optic filter designs, and inverse scattering problems.

Lei Zhu (S'91–M'93–SM'00–F'12) received the B.Eng. and M.Eng. degrees in radio engineering from Southeast University, Nanjing, China, in 1985 and 1988, respectively, and the Ph.D. degree in electronics engineering from the University of Electro-Communications, Tokyo, Japan, in 1993.

He was a Research Engineer with Matsushita-Kotobuki Electronics Industries Ltd., Tokyo, from 1993 to 1996. From 1996 to 2000, he was a Research Fellow with the École Polytechnique de Montréal, Montréal, QC, Canada. From 2000 to 2013, he was an Associate Professor with the School of Electrical and Electronic Engineering, Nanyang Technological University, Singapore. Since 2013, he has been a Full Professor with the Faculty of Science and Technology, University of Macau, Macau, China. Since 2014, he has been serving as the Head of the Department of Electrical and Computer Engineering, with the University of Macau. So far, he has authored or co-authored more than 310 papers in international journals and conference proceedings. His papers have been cited more than 3700 times with an H-index of 33 (ISI Web of Science). His current research interests include microwave circuits, guided-wave periodic structures, antennas, and computational electromagnetic techniques.

Dr. Zhu was a recipient of the 1997 Asia-Pacific Microwave Prize Award, the 1996 Silver Award of Excellent Invention from Matsushita-Kotobuki Electronics Industries Ltd., and the 1993 First-Order Achievement Award in Science and Technology from the National Education Committee, China. He was the Associate Editor of the IEEE TRANSACTIONS ON MICROWAVE THEORY AND TECHNIQUES from 2010 to 2013 and the IEEE MICROWAVE AND WIRELESS COMPONENTS LETTERS from 2006 to 2012. He served as a General Chair of the 2008 IEEE MTT-S International Microwave Workshop Series on the Art of Miniaturizing RF and Microwave Passive Components, Chengdu, China, and a Technical Program Committee Co-Chair of the 2009 Asia-Pacific Microwave Conference, Singapore. He served as the member of the IEEE MTT-S Fellow Evaluation Committee from 2013 to 2015, and has been serving as the member of the IEEE AP-S Fellows Committee since 2015.